Pak, V. & Hashmi, J.A. (2023). Top-down threat bias in pain perception is predicted by higher segregation between restingstate networks. *Network Neuroscience*, Advance publication. https://doi.org/10.1162/netn_a_00328.

Title: Top-down threat bias in pain perception is predicted by higher segregation between resting-state networks

Short title: High system segregation in RSNs predicts top-down threat bias.

Authors: Veronika Pak[1,2], Javeria Ali Hashmi[3,4]

[1]Department of Neurology and Neurosurgery, McGill University, Montreal, Canada

[2]McConnell Brain Imaging Centre, Montreal Neurological Institute, Montreal, Canada

[3]Department of Anesthesia, Pain Management, and Perioperative Medicine, Nova Scotia Health Authority, Halifax, NS, Canada

[4]Dalhousie University, Halifax, NS, Canada

ABSTRACT

Top-down processes such as expectations have a strong influence on pain perception. Predicted threat of impending pain can affect perceived pain even more than the actual intensity of a noxious event. This type of threat bias in pain perception is associated with fear of pain and low pain tolerance and hence the extent of bias varies between individuals. Large-scale patterns of functional brain connectivity are important for integrating expectations with sensory data. Greater integration is necessary for sensory integration hence, here we investigate the association between system segregation and top-down threat bias in healthy individuals. We show that top-down threat bias is predicted by less functional connectivity between resting-state networks. This effect was significant at a wide range of network thresholds and specifically in pre-defined parcellations of resting-state networks. Greater system segregation in brain networks also predicted higher anxiety

and pain catastrophizing. These findings highlight the role of integration in brain networks in mediating threat bias in pain perception.

Keywords: pain perception, bias, top-down, expectation, prediction, threat, functional MRI, functional connectivity, system segregation, resting-state networks, pain catastrophizing

INTRODUCTION

Any painful experience aids the learning of threat contingencies so that future experiences of pain can be inferred, and tissue damage can be prevented. These top-down processes, through which expectations influence pain, may rely on brain network architecture (Caras & Sanes, 2017; Choi et al., 2018). Parsing out individual differences in large-scale network features that govern pain perception and how expectations modulate pain intensity can be useful for understanding why people perceive pain differently and what goes awry in chronic pain conditions (Fields, 2018; Heathcote et al., 2020; Leeuw et al., 2007; Peters et al., 2002).

When a sensory experience relies more on prediction and less on sensory verification, the result is a biased perceptual experience that deviates from the objectively defined external cause. A key function of pain is to warn and direct attention towards threats (Kucyi & Davis, 2015; Legrain et al., 2011). Hence, in pain averse individuals, expectations can have a strong hold on perception when noxious events are expected to be more intense (Aue & Okon-Singer, 2015; Bar-Haim et al., 2007; Kelley & Schmeichel, 2014; LeDoux, 2014; Smith et al., 2021). We have reported that a stepped increase in the threat of experiencing a strong pain evoking stimulus can significantly magnify the pain even though the stimulus intensity was constant (Lim et al., 2020).

Each cued increase in the expected stimulus strength, linearly increased the perceived pain intensity (Kong et al., 2013; Lim et al., 2020). In some individuals, the increased threat of strong noxious stimuli produced increasingly more intense pain and this variability was taken as an indicator of top-down threat bias (Aristi et al., 2022). Greater threat bias was predicted by higher pain catastrophizing scores, low mindful awareness, low pain tolerance (Lim et al., 2020), and was also associated with reduced integrity in white matter pathways needed in the brain for sensory and top-down integration (Aristi et al., 2022). Nevertheless, the effects of variability in large-scale functional connectivity patterns on pain perception remain unknown.

Brain networks consist of modules representing sub-networks where each may putatively serve distinct functions (Gozdas et al., 2019; Khan et al., 2022; Rubinov & Sporns, 2010; van den Heuvel & Sporns, 2013). These modules are in turn connected with each other through relatively sparse global connections (Baum et al., 2017). The balance of the number of connections within and between sub-networks, termed as system segregation/integration (SS), varies between individuals and is a useful feature that captures higher-order cognitive brain functions (Cohen & D'Esposito, 2016; Misic & Sporns, 2016). It has been suggested that system integration in brain networks reflects cognitive efforts and has been also shown to predict performance accuracy in a working memory task (Cohen & D'Esposito, 2016). In contrast, greater clustering and more system segregation predicted the ability to adhere to prescribed training such as meditation, cognitive behavioral therapy and exercise (Arnemann et al., 2015; Baniqued et al., 2019; Baniqued et al., 2017; Gallen et al., 2016; Saghayi et al., 2020). Although, any specific function of network segregation is unclear, putatively, brain sub-networks that function relatively independently may have increased capacity for specialized functions but at the possible cost of a reduced capacity to

integrate new information (Aristi et al., 2022; Bullmore & Sporns, 2012; Hashmi et al., 2017). For instance, higher clustering indices, which is a measure related to SS, has been reported to predict higher expectation effects towards the efficacy of a treatment (placebo analgesia) (Hashmi et al., 2014). Note that when placebo analgesia and expectation effects are strong, they can be represented as a type of cognitive bias, where the error between actual and predicted sensation are not fully integrated and perception is more reliant on the top-down priors. This type of bias may be associated with individual differences in the capacity to integrate information from different subnetworks in the brain, but a direct mapping between top-down expectation effects and SS is yet to be clearly demonstrated.

Here we investigate top-down threat bias in healthy individuals at a wide range of network thresholds. We test reproducibility with three different a priori brain parcellations, (i.e. previously predefined), and also with subject-specific parcellations. Results were verified by analyzing association with threat bias values as a continuous variable and also by grouping individuals into high and low bias groups. To further explore the role of SS in mediating group differences in threat bias, we studied the change in SS between rest and task. In addition, we tested the interrelationship between the brain measures and relevant variables including age, pain catastrophization, and anxiety.

MATERIALS AND METHODS

Participants. Forty-two healthy and right-handed individuals (21 female; ages 20-56 years; mean age ± SD of 31.23 ± 10.91 years) were recruited for the study and provided written informed consent. Exclusions criteria were as follows: (1) having concomitant acute or chronic pain; (2)

taking medications for pain; (3) pregnancy; (4) history of cardiac, respiratory, or nervous system disease that could interfere with participation in the study or present potential for adverse outcome (e.g., asthma or psychiatric or mental disorders); or (5) contraindications to MRI scanning [e.g., cardiac pacemaker, metal implants (including titanium), dental braces, permanent retainers, or known fear of closed spaces]. The study protocol was approved by the Nova Scotia Health Authority Research Ethics Board.

Of all 42 participants, 39 underwent structural T1-weighted MRI, diffusion-weighted imaging (DWI), functional MRI (fMRI) resting-state scan, and experimental pain task scans. The analysis of this study focuses on resting-state and experimental fMRI data collected from 39 participants. On structural analyses made on this dataset, see our previously reported findings (Aristi et al., 2022; Lim et al., 2020; Wang et al., 2022).

Pain task experiment. The task was designed as a cognitive test of bias to evaluate the influence of top-down threat predictions on new sensory experience. Before proceeding to the MRI scanner, participants were informed that they would be shown information on a screen, experience thermal stimuli (heat), and be asked to rate the experienced pain intensity using a numeric scale.

Each trial, threat cues on the screen would either predict the stimulus intensity in the form of a percentage range of 10 points (example: "the incoming heat stimulus is at 70-80% intensity") or prompt that the stimulus intensity is unknown ("the incoming heat stimulus intensity is unknown"). While participants were looking at a red fixation cross on the screen, the heat stimulation was delivered to their skin on their lower left leg (*tibialis anterior muscle*) via an ATS

30 × 30 mm thermode (PATHWAY system, Medoc). Participants were asked to rate their perceived pain intensity by using a 0-100 numerical rating scale (NRS; where 0 means no pain at all and 100 being the worst pain imaginable). Participants moved the cursor along the scale to select a number representing their pain level by pressing two buttons on an MRI-compatible response pad (Lumina LSC-400 controller, Cedrus). For a graphical representation of the task, see Figure 1A.

The procedure described above was repeated multiple times across four different runs including one matched-condition run, one level 1 mismatched-condition run, and two level 2 mismatched-condition runs. Mismatched runs were shortly named task 1, task 2a and task 2b, respectively.

In the matched run (see Figure 1B), threat cue values accurately predicted pain intensities in a linear fashion. Each 10-point increase in cued threat value was associated with a 0.4° increase in stimulus temperature (43.8–47°C temperature range). Therefore, during the matched condition, participants were taught to anticipate pain intensity based on the correctly predicted level of threat.

In mismatched runs, threat cue values did not match the following heat stimuli, introducing the difference between expected and actual stimulus intensities. Three mismatched condition runs were conducted to determine whether the linear relationship learnt by participants during the matched condition carried over to subsequent runs of the task, followed. During the level 1 mismatched run, all cue values ranging from 1-40% were coupled with the same low-heat 45°C stimulus and cue values ranging from 60-100% were paired with a high heat 47°C stimulus. There

was no prediction error for cue ranges of 31-40% and 91-100%. In the remaining level 2 mismatched runs, all threat cue values were paired with the maximum temperature of 45 °C or a 47°C. Participant's reliance on the information presented by the visual cues, i.e., their top-down bias, was measured using the trials in level 2 runs where the temperature was always 47 °C (Figure 1C). The top-down threat bias was thus assessed by measuring the difference in pain ratings between the high and low threats cues, when the stimulus temperature remained the same in each participant.

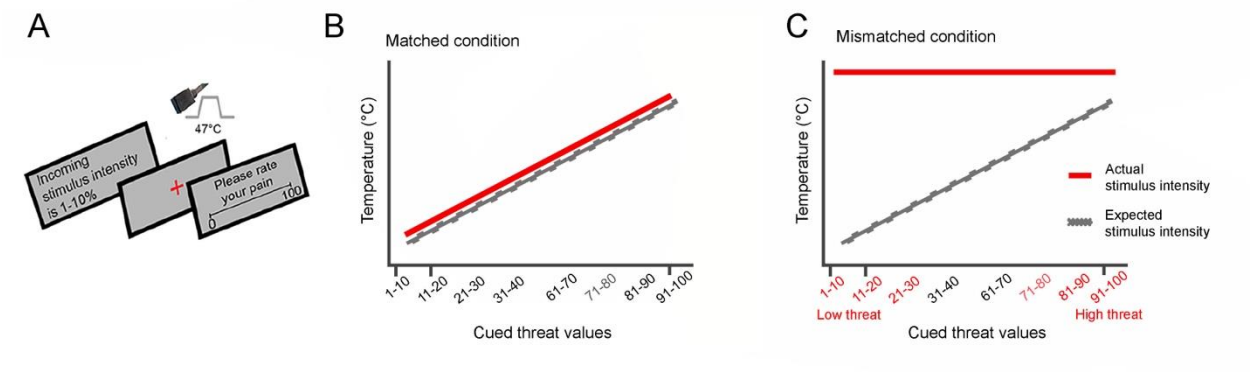

Figure 1. Experimental paradigm of the pain task performed by participants during fMRI acquisition. **A.** In each trial, a threat cue stating the intensity of the incoming stimulus was shown on the screen. Heat pain stimulus was administered during the presentation of a red fixation cross on the screen. Then, participants were asked to rate their pain intensity on a scale of 0–100. **B.** Matched condition: threat cue predictions matched the heat stimuli intensity in a linear fashion, thus training participants to learn a linear schema on perceived pain, where actual stimulus intensity matched the expectations of the perceived pain. **C.** Mismatched condition: in the last two runs (task 2a and 2b), all threat cues were coupled with the maximum heat temperature of 47°C, as depicted on the plot. High threat cue values ranged from 70 to 98 and low threat cue values

ranged from 8 to 32. The difference between pain ratings for high threat cues and low threat cues during the mismatched run was defined as top-down threat bias.

Top-down threat bias calculation. Effect of top-down threat cues on pain perception was calculated as a difference between averaged pain ratings in response to the low threat cue values (8-32%) and to the maximum cue values (70-98%). A greater difference indicated a stronger effect of threat cues on pain ratings. Only data collected during the mismatched level 2 runs, when the temperature remained at its peak (47 °C) throughout the task, was used in these calculations.

We conducted a group comparison of individuals with different levels of threat bias to verify the results where threat bias was used as a continuous variable. Participants were assigned to the low threat bias (n = 15) and high threat bias (n = 17) groups by using a K-means clustering algorithm implemented in MATLAB (Lloyd, 1982). The algorithm assigned cluster memberships based on the data distribution itself and with minimal user decision-making. High threat bias group included participants whose pain perception was more aligned with threat expectation and less with the actual heat stimulus. Participants that were being reclassified after each iteration (n = 7) and whose bias fell near the mean of the distribution were excluded from the group analysis.

Psychosocial measures. The pain catastrophizing scores and its three subscales (Rumination, Magnification and Helplessness) were obtained using the Pain Catastrophizing Scale (PCS) questionnaire (Sullivan et al., 1995). State anxiety and trait anxiety were evaluated by self-reported The State-Trait Anxiety Inventory (STAI) (Spielberger et al., 1970).

Data Acquisition. Structural and functional scans were collected using a 3T MRI scanner (Discovery MR750; General Electric Medical Systems, Waukesha, WI, USA) with a 32-channel head coil (MR Instruments, Inc.; Minneapolis, MN, USA). The experiment took place at the Halifax Infirmary Site, QEII Health Sciences Centre, Halifax, NS, Canada. Participants' heads were fitted with foam padding to provide comfort and minimize motion, ear plugs were used to reduce sound levels, and reminders were given before each scan to keep their head still. Resting-state scan lasted 8 minutes. The following parameters were used for T1-weighted brain images (GE sequence 3D IR-FSPGR): field of view = 224×224 mm; in-plane resolution = 1mm×1mm; slice thickness = 1.0mm; TR/TE = 4.4/1.908 milliseconds; flip angle = 9°. The fMRI BOLD (blood oxygenation level dependent) sequence protocol used a multi-band EPI sequence: field of view = 216×216 mm; in-plane resolution = 3mm×3mm; slice thickness=3.0mm; TR/TE=950/30 milliseconds, SENSE factor of 2, acceleration factor of 3. There were 500 volumes for resting-state scans, 814 volumes for the training scan (not used in analysis), and 624 for the three pain task scans in total. For distortion correction, reverse phase encoded images were also obtained for the application of FSL's topup.

Preprocessing of resting-state data. All functional datasets were corrected for field map-based distortion. Data were preprocessed with AFNI (http://afni.nimh.nih.gov/afni) and FSL (http://www.fmrib.ox.ac.uk/fsl), with the scripts provided by 1000 Functional Connectomes Project (http://www.nitrc.org/projects/fcon_1000). All the following parameters for preprocessing were adapted from the parent study (Lim et al., 2020). Preprocessing with AFNI included (1) discarding the first five EPI volumes to allow signals to reach a steady state, (2) rigid-body motion correction of time series by aligning each volume to the mean image using Fourier interpolation,

(3) skull stripping, and (4) getting an eighth image for use in registration. Preprocessing using FSL consisted of (5) spatial smoothing with a Gaussian kernel of full-width half-maximum=6 mm, (6) grand-mean scaling of the voxel value, (7) bandpass temporal filtering between 0.005 and 0.3Hz, (8) removal of linear and quadratic trends using Fourier transformation, and (9) mean-based intensity normalization.

The six motion parameters corresponding to rotational movement and cardinal displacement were generated using the FSL-based motion correction step in native functional space. In addition, two nuisance time courses were calculated for white matter and ventricles by using masks obtained from the image segmentation of the participant's T1w data and applying a tissue-type probability threshold of 80%.

For analyzing data in standard space, FLIRT was used to perform registration of functional images to the MNI152 standard template (Fonov et al., 2011). This included (1) registration of native-space structural image to the MNI152 2mm template using twelve df linear affine transformation, (2) registration of native-space functional image to high-resolution structural image with six df linear transformation, and (3) computation of native-functional-to-standard-structural warps using by concatenating matrices computed in steps (1) and (2).

For data quality verification, maximum framewise displacement (FD) and DVARS (difference of volume N to N+1), were calculated to assess motion. For image quality criteria, participant data with maximum FD above 3mm or DVARS outliers detected in more than 10% of the acquired data were removed from analysis. Mean FD was 0.12 (SD=0.07) and mean DVARS

was 46.9 (SD=4.7). No images were excluded, as the highest maximum FD obtained and highest percentage of outliers in data detected for all participants was 2.65 mm and 8%. Maximum FD and maximum DVARS were used as nuisance covariates when correlating functional and behavioral metrics for further verification.

Brain parcellations. For each participant, image voxels were grouped into 131 regions of interest (ROIs), which were defined by the optimized Harvard-Oxford atlas for pain studies (Hashmi et al., 2014; Saghayi et al., 2020). BOLD time series were extracted from each voxel within each region and then averaged using FSL. The regions were grouped within the following five canonical resting-state networks: subcortical, sensory, default mode, attention/executive, and language/memory (Hashmi et al., 2017).

Additional group-level parcellations with seven and seventeen resting-state networks were employed from the open-source Yeo atlas (Yeo et al., 2011). Seven network parcellation included 52 ROIs and the seventeen network parcellation included 114 ROIs. Seven networks spanned visual, somatomotor, dorsal attention, ventral attention, limbic, frontoparietal, and default mode networks. The seventeen networks presented a higher resolution extended parcellation with inclusion of sensory and motor cortices (Yeo et al., 2011). These estimated networks have been chosen for showing reliability across datasets and being previously validated in region-based fMRI analyses (Yeo et al., 2011; Zhi et al., 2022).

System segregation calculation. Whole brain weighted system segregation was measured with a graph theory technique. To build the functional connectivity graph, the 131x131 adjacency matrix for each participant was created by calculating zero-lag Pearson's linear correlations between the

131 BOLD time series. Negative correlation values and diagonal entries were removed from the correlation matrices. For selecting only significant functional connections unaffected by physiological or experimental noise, each matrix was thresholded and converted to a binarized adjacency matrix (van Wijk et al., 2010). Network thresholding was based on predefined correlation thresholds (percentage of the strongest connections) ranging from 0.20 to 0.5, with increment of 0.05. This range of possible thresholds was used to test for consistency of the results to account for spurious connections in unthresholded networks. Moreover, there is no consensus regarding an optimal threshold and removing some connections may lead to the loss of important information at the cost of reduced sensitivity (Drakesmith et al., 2015; van den Heuvel et al., 2017; Zalesky et al., 2016). We used functions from the Brain Connectivity Toolbox and custom code implemented in MATLAB to quantify functional networks from the matrix (Avena-Koenigsberger et al., 2017; Rubinov & Sporns, 2010).

A measure for weighted system segregation for each network was defined as the difference between mean Fisher's z-transformed within-network connectivity and mean Fisher's z-transformed between-network connectivity and was calculated by the following formula:

$$System\ segregation = \frac{\bar{z}_w - \bar{z}_b}{\bar{z}_w},$$

where $\bar{z}_w$ is the number of connections within a given network and $\bar{z}_b$ is the number of connections between nodes (ROIs) within a given network and other networks, normalized by the total number of possible connections between networks. The code for the measure was employed from the study of Chan et al. (2014).

Subject-specific system segregation calculation. We defined subject-specific networks by adopting Girvan-Newman and Louvain algorithms, commonly used methods for community detection (Braga & Buckner, 2017; Harrison et al., 2015; Laumann et al., 2015; Yeo et al., 2011). This approach known as modularity maximization process that aims to partition network's nodes into brain modules (networks) (Sporns & Betzel, 2016). Specifically, we calculated subject-specific weighted system segregation between a set of non-overlapping modules (*m* as the total number of modules) calculated by the following formulas:

$$Q = \frac{1}{2m}\sum_{i,j}\left[A_{ij} - P_{ij}\right]\delta\left(c_i, c_j\right),$$

where Q is a modularity coefficient, A_{ij} represents the number of connections between nodes i and j, c_i and c_j are the networks to which nodes *i* and *j* belong, *m* is the sum of all connectivity weights in the graph, δ is the Kronecker delta function, and P_{ij} stands for the expected number of connections according to a null model (Newman & Girvan, 2004). For an undirected network based on the Louvain method, the following formula was applied:

$$Q = \frac{1}{2m}\sum_{i,j}\left[A_{ij} - \frac{k_i k_j}{2m}\right]\delta\left(c_i, c_j\right),$$

where $P_{ij} = \frac{k_i k_j}{2m}$, k_i and k_j are the sum of the connectivity weights attached to nodes *i* and *j*, and the delta-function $\delta\left(c_i, c_j\right)$ equals 1 if *i* = *j* and 0. Otherwise, $2m = \sum_{ij} A_{ij}$ is the total number of connections in the network (Blondel et al., 2008).

RESULTS

Cue threat predictions altered pain perception evoked by a heat stimulus

As we have previously reported, presenting threat predictions as cues prior to applying heat stimuli significantly influenced pain perception in healthy participants (Lim et al., 2020). Figure 2A demonstrates averaged pain ratings in response to low threat cues (8-32) and high threat cues (70-98) averaged from three mismatched runs. These differences in pain ratings were related to the cues since in both conditions the stimuli were identical (peak stimuli intensity of 47°C), indicating the effect of linear schema on pain perception i.e. top-down threat bias. A greater difference in pain ratings was suggestive of a stronger top-down threat bias.

Figure 2B shows the distribution of bias scores calculated for 39 participants (-25.03 ± 15.86) as a difference in pain ratings in mismatched runs between low threat cues and high threat cues. The median of the distribution (-25) was within 10% of the mean, suggesting that the variability was normally distributed ($W = 0.953$, $p = 103$). K-means clustering was used to assign participants into two groups (high bias, n = 17; low bias, n = 15) based on their threat bias scores (high bias -40.2, ± 8.31; low bias, -8.56 ± 5.4). The high bias group included individuals whose pain perception became intensified with increase in threat of a stronger stimulus. We have previously reported significant influence of all cue values on pain ratings in both threat groups (Aristi et al., 2022). Specifically, the increase in reported pain with increase in cued threat was more steep in the high bias group, while ratings in the low bias group showed less amplification with increase in cued threat (Aristi et al., 2022).

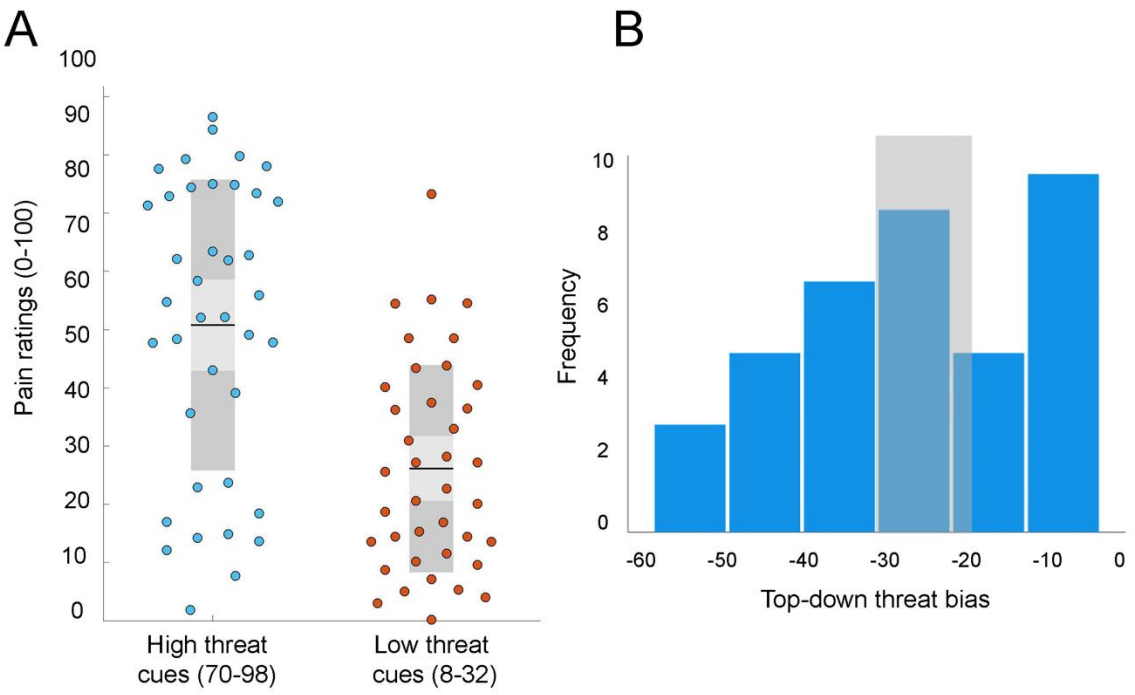

Figure 2. (A) Effects of high threat (70-98) and low threat (8-32) cue values on participants' pain ratings during mismatched conditions. Pain ratings for high threat cues were significantly altered by threat bias formed by the linear schema. (B) Frequency distribution of perceptual threat bias scores calculated for healthy participants. The values for all participants were used as a continuous variable for testing associations with system segregation. For group analysis, participants lying on the left (n = 17) and right (n = 15) sides were classified by K-mean clustering algorithms into the high threat bias and low threat bias groups, respectively. Shaded region shows the cut-off band of the K-means classification, where participants that lie within the band (n = 7) were excluded from the group analysis.

System segregation during rest predicts top-down threat bias

We first tested whether SS in five functional RSNs predicted top-down threat bias in 39 healthy individuals that underwent fMRI scans. We also compared differences in SS between individuals

from the high bias and low bias groups. In addition we tested if the findings reproduce when two other parcellations with different spatial resolutions from the Yeo atlas (Yeo et al., 2011) were used.

As Figure 3 illustrates, higher weighted SS in five networks significantly correlated with higher top-down threat bias in pain perception at all seven sparsity thresholds ($T^{0.20\text{-}0.50}$: R = -0.412, p = 0.009; R = -0.390, p = 0.014; R = -0.378, p = 0.018; R = -0.376, p = 0.018; R = -0.371, p = 0.02; R = -0.370, p = 0.02; R = -0.375, p = 0.019; Figure 3A). These findings were reproducible in seven networks: SS significantly correlated with threat bias at six out of seven sparsity thresholds ($T^{0.20\text{-}0.45}$: R = -0.358, p = 0.025; R = -0.334, p = 0.038; R = -0.338, p = 0.035; R = -0.336, p = 0.037; R = -0.328, p = 0.041; R = -0.319, p = 0.048; Figure 3B). In comparison, the correlation analysis did not show significant correlations between threat bias and SS in seventeen networks (p>0.05). While results were not significant relative to the standard alpha level of .05, the p-value was less than .10 at all sparsity thresholds. This result suggests that SS in seventeen networks showed a trend similar to the findings from other parcellations and indicated that parcellations with lower spatial resolution were more effective in capturing the association between segregation and the threat bias (Figure 3C).

In group analysis, we found a significant between-subjects effect (RM-ANOVA: F(1) = 4.816, p = 0.036) on SS in five canonical RSNs. This effect was reproducible in seven networks (RM-ANOVA: F(1) = 5.224, p = 0.030) and in seventeen (RM-ANOVA: F(1) = 5.115, p = 0.031). Post-hoc analysis showed that weighed SS in five networks was significantly different between the high threat bias and low threat bias groups at all seven sparsity thresholds ($T^{0.20\text{-}0.50}$: t = -2.348,

p = 0.026; t = -2.22, p = 0.034; t = -2.156, p = 0.039, t = -2.168, p = 0.038; t = -2.122, p = 0.042; t = -2.131, p = 0.041; t = -2.167, p = 0.038; independent t-test, Figure 3D). Other parcellation networks produced similar results: the high bias group showed higher SS compared to the low bias group at all seven sparsity thresholds in seven networks ($T^{0.20\text{-}0.50}$: t = -2.497, p = 0.018; t = -2.31, p = 0.028; t = -2.366, p = 0.025, t = -2.289, p = 0.029; t = -2.217, p = 0.034, t = -2.134, p = 0.041; t = -2.067, p = 0.047; independent t-test, Figure 3E) and at all seven sparsity thresholds in seventeen networks ($T^{0.20\text{-}0.50}$: t = -2.284, p = 0.03; t = -2.337, p = 0.026; t = -2.257, p = 0.031; t = -2.235, p = 0.033; t = -2.263, p = 0.031; t = -2.226, p = 0.034; t = -2.196, p = 0.036; independent t-test, Figure 3F). In the explorative analysis, we found that the high bias group showed more functional connectivity within RSNs. In comparison, the low bias group, showed a larger number of significant connections between RSNs. These exploratory results illustrate that the high bias group shows greater SS relative to the low bias group (Supplementary Figure 1).

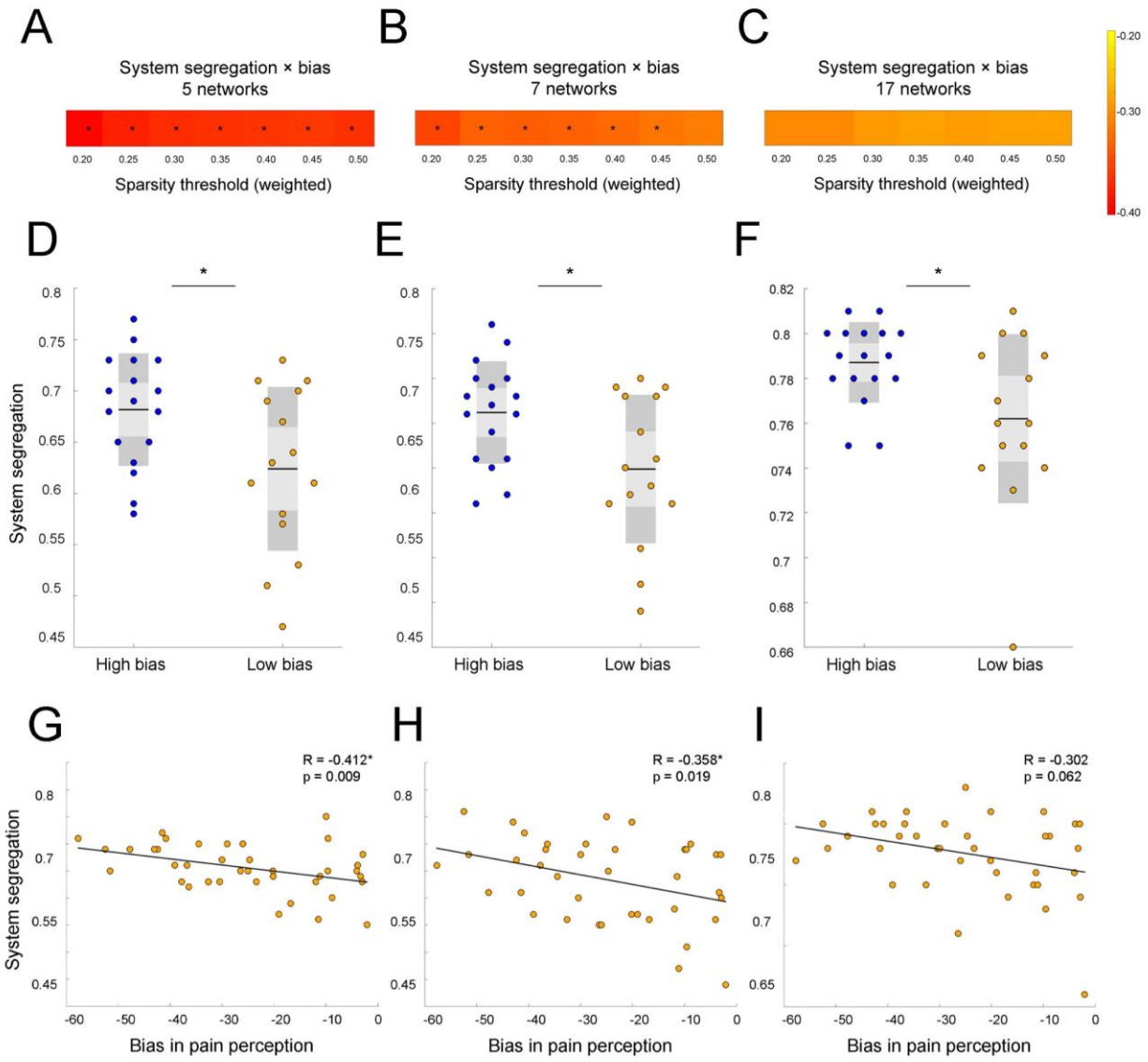

Figure 3. System segregation during resting-state predicts top-down threat bias in pain perception at a wide range of network thresholds when tested with three different brain parcellations. (A) SS in five networks significantly correlates with threat bias at all sparsity thresholds ($p < 0.05$). (B) In seven networks, SS is associated with bias at almost all thresholds ($p < 0.05$). (C) A similar trend towards significance can be observed for correlations in seventeen networks. The heat map on the right demonstrates the R values ranging from -0.2 (colored yellow) to -0.4 (red) for all parcellation schemes. (D-F) Participants in the high bias group demonstrated significantly higher

SS compared to the low bias group at the 0.20 threshold ($p = 0.026$; $p = 0.018$; $p = 0.03$). Between-subjects effect was significant for all parcellations ($p < 0.05$). (G) Scatter plot demonstrates a significant negative relationship between SS in five networks and threat bias at the 0.20 threshold ($p = 0.009$). (H) SS in seven networks also decreases with threat bias at the 0.20 threshold ($p = 0.019$) (I) Similar trend of a negative association between SS and threat bias can be observed in seventeen networks at the 0.20 threshold. For each scatterplot, a line reflecting a linear regression between SS and threat bias in pain perception is depicted. Significant results are marked by asterisks (*).

Subject specific parcellations and system segregation

Girman-Newman and Louvain algorithms for community detection were utilized to identify the number of network communities for each subject individually (Blondel et al., 2008; Newman & Girvan, 2004). Compared to the results from the predefined networks (optimized Harvard Oxford and Yeo), weighted SS measured from subject-specific modules by the Girvan-Newman algorithm significantly correlated with top-down bias at only one sparsity threshold ($T^{0.20}$: $R = -0.337$, $p = 0.036$). Correlations between subject-specific weighted SS based on the Louvain method were not significant at any of the sparsity thresholds.

Changes in segregation of functional brain networks from rest-to-task

Figure 4 illustrates changes in SS values averaged across participants between resting-state scan and mismatched runs of the pain schema task. Two types of analysis were run. First, we looked at overall changes in SS with tasks, for that we looked at whether SS significantly changes with each subsequent scan. The RM-ANOVA revealed a significant overall effect on SS for all participants

(F(18) = 4.968, $p < 0.01$ for type of scan x threshold). However, the between-subjects effect was not significant (F(1) = 3.315, p = 0.079). The variability in SS between scans was not significant for the low bias group (F(27) = 1.347, p = 0.118 for type of scan x threshold; Figure 4C). Meanwhile, participants in the high bias group showed significant changes in SS from rest-to-task scans (type of scan x threshold, F(27) = 482.709, $p < 0.01$). Effect of the type of scan alone was also significant (F(3) = 478.572, $p < 0.01$). Figure 4D demonstrates how integration across 5 networks increases gradually with each task for the high bias group.

Post-hoc analysis showed that significant changes occurred mainly between task1 and task 2b across five out seven sparsity thresholds ($T^{0.20\text{-}0.40}$: t = 2.429, p = 0.028; t = 2.43, p = 0.028; t = 2.335, p = 0.034; t = 2.318, p = 0.035; t = 2.345; p = 0.033). There was no significant difference in the prediction errors in task 2a and 2b (Lim et al., 2020). Given that there was no change in task condition between these tasks, the lack of changes in SS indicated that prediction errors played a role only in changes observed between other scans. To test this assumption the overall model was run without task 2b and showed stronger effect (RM-ANOVA: F(12) = 5.563, $p < 0.01$ for type of scan X threshold). The between subject effect was significant (F(1) = 4.739, p = 0.037).

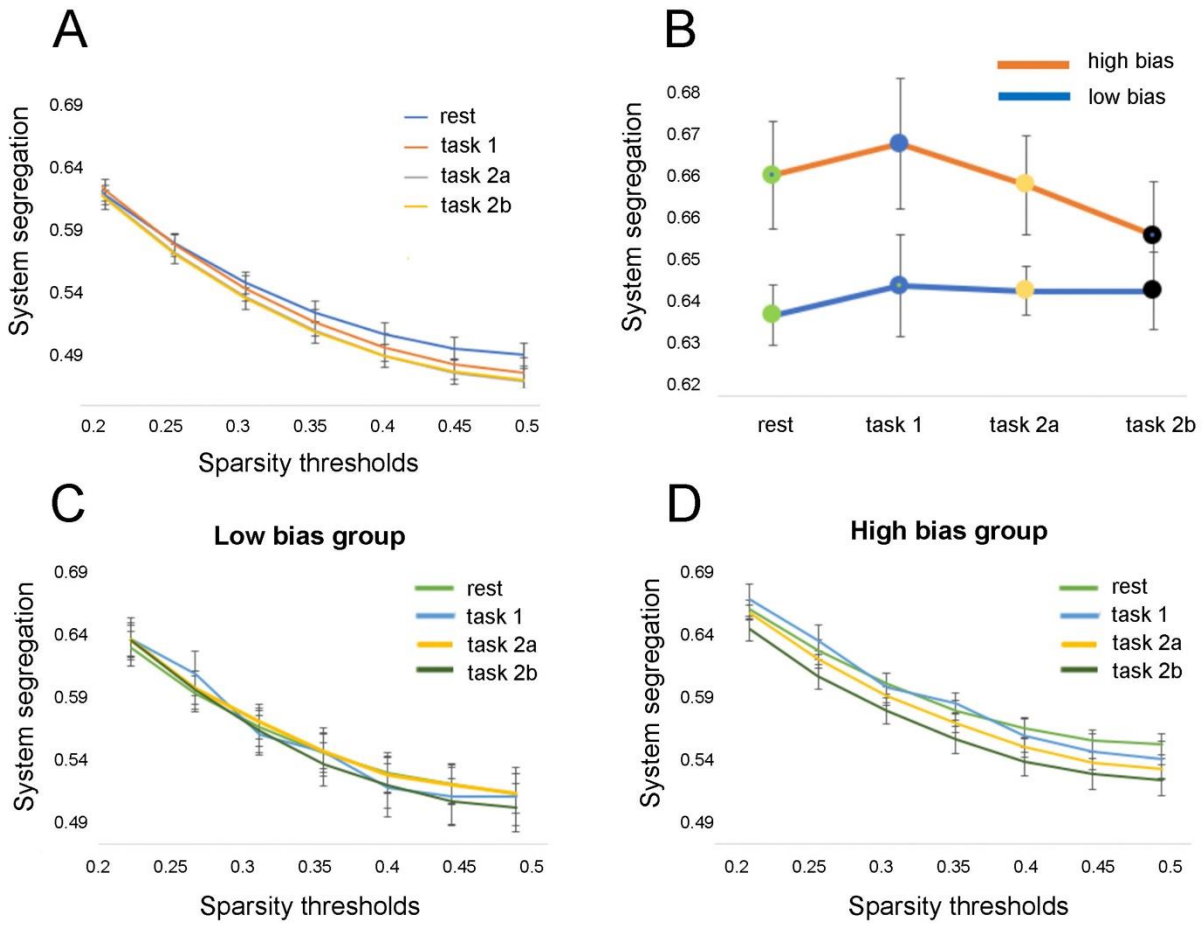

Figure 4. Participants in the high threat bias group showed significant changes in system segregation from rest-to-task scans compared to people in the low threat bias group. (A) Variability in SS values from rest-to-task showed significant interaction effect for type of scan and a sparsity threshold value ($p < 0.01$). (B) Participants in the high bias group showed significantly higher SS during rest, tasks 1, and 2a compared to the low bias group at the 0.20 threshold (RM-ANOVA: $p < 0.05$). (C) No variation in SS from rest-to-task in the low bias group was identified across all sparsity thresholds (RM-ANOVA: $p = 0.118$). (D) Significant changes in SS between resting-state and task scans were observed in high bias group at different sparsity thresholds (RM-ANOVA: $p < 0.01$).

Relationships between segregation in networks and demographic characteristics

To measure the effect of maladaptive characteristics related to pain, the relationships between SS and self-reported pain catastrophizing, anxiety and depression measures were investigated.

Table 1 summarizes what demographic metrics were used and how they were associated with segregation in RSNs defined by different parcellations at the 0.20 sparsity threshold. Next, we report correlations that were significant at most sparsity thresholds only. Higher SS between five networks predicted higher magnification, an aspect of pain catastrophizing, at all seven sparsity thresholds ($T^{0.20\text{-}0.50}$: R = 0.435, p = 0.006; R = 0.407, p = 0.01; R = 0.390, p = 0.014; R = 0.381, p = 0.017; R = 0.369, p = 0.021; R = 0.360, p = 0.024; R = 0.352, p = 0.028). In 17 networks, decreased integration was a significant indicator of state anxiety ($T^{0.20\text{-}0.50}$: R = 0.371, p = 0.02; R = 0.396, p = 0.013; R = 0.388, p = 0.015; R = 0.392, p = 0.014; R = 0.384, p = 0.016; R = 0.377, p = 0.018; R = 0.369, p = 0.021) and trait anxiety ($T^{0.20\text{-}0.50}$: R = 0.376, p = 0.018; R = 0.392, p = 0.014; R = 0.380, p = 0.017; R = 0.385, p = 0.015; R = 0.379, p = 0.017; R = 0.377, p = 0.018; R = 0.371, p = 0.02) at all seven sparsity thresholds.

Table 1. Relationship between system segregation and demographic characteristics for healthy controls (*n* = 39) at the 0.20 weighted threshold.

Parameters	Mean ± STD	R value			p value		
Networks		Five	Seven	Seventeen	Five	Seven	Seventeen
Age[x]	31.41 ± 10.17	-0.291	-0.104	-0.251	0.073	0.527	0.123
PCS	12.44 ± 9.99	0.316*	0.261	0.219	0.05	0.109	0.18

Rumination[x]	5.54 ± 4.84	0.269	0.162	0.122	0.098	0.326	0.461
Magnification	2.82 ± 2.39	0.435*	0.196	0.166	0.006	0.231	0.313
Helplessness[x]	4.69 ± 4.68	0.177	0.291	0.243	0.281	0.072	0.136
State anxiety	32.18 ± 9.66	0.119	0.264	0.371*	0.505	0.104	0.020
Trait anxiety	35.80 ± 10.40	0.155	0.323*	0.376*	0.345	0.045	0.018

Significant correlations are defined by asterisks (*). [x] indicates that non-parametric Spearman's correlation analysis was performed on data instead of Pearson since data was not normally distributed.

We assessed sex differences in top-down threat bias and weighted SS at different thresholds. There were no significant differences between male and female participants in threat bias ($p = 0.574$) and in SS ($T^{0.20\text{-}0.50}$: $p = 0.366$; $p = 0.254$; $p = 0.188$; $p = 0.151$; $p = 0.130$; $p = 0.111$; $p = 0.094$). In addition, we confirmed that the group differences in SS were not related to head motion. We did not observe a significant difference in maximum frame wise displacement (FD) and DVARS between the high and low bias groups for all the three network parcellations ($p>0.05$). Similarly, there was no significant correlation between these two motion metrics and SS ($p>0.05$).

DISCUSSION

Here we report that higher segregation in RSNs was associated with greater amplification in pain during manipulated expectations of a stronger pain stimulus. Higher segregation in functional brain

networks also associated with higher anxiety and pain catastrophizing. Our findings were reproducible at a wide range of network sparsity thresholds and between different types of pre-defined parcellations but were not significant when were tested with subject-specific parcellations.

Both segregation and integration of brain networks have been recognized to be critical for cognitive functioning (Cohen & D'Esposito, 2016; Deco et al., 2015; Friston, 2009; Sporns, 2013; Wig, 2017). Previous work has shown that higher SS predicts different types of cognitive capacities and the ability to learn new physical and mental skills such as cognitive behavioral therapy and meditation (Arnemann et al., 2015; Baniqued et al., 2019; Baniqued et al., 2017; Cohen & D'Esposito, 2016; Gallen et al., 2016; Saghayi et al., 2020). More segregated networks also predicted higher expectation effects of placebo analgesia suggesting the role of segregation in the process of integrating top-down information with sensory input (Hashmi et al., 2014). In the present study, we have found that higher segregation between canonical RSNs is associated with a top-down bias (or reduced capacity to integrate sensory evidence).

It has been suggested that individuals can vary in SS due to underlying differences in neurotransmitter functions. A prominent hypothesis suggests that large-scale network dynamics are mediated by neuromodulatory neurotransmitter inputs from the ascending arousal system (Shine, 2019; Shine et al., 2018; Shine et al., 2016; Shine et al., 2019). Specifically, it has been shown that widespread projections from the noradrenergic locus coeruleus (LC) coordinate neural gain which in turn affects the balance between segregation and integration by altering network level topology to promote attentional and cognitive performance (Shine et al., 2018; Wainstein et al., 2021). In addition, the patterns of segregation and integration are correlated with the spatial

distribution of the α2a adrenergic receptors (Wainstein et al., 2021). We have previously demonstrated that α2 adrenergic receptors are important for maintaining brain network architecture by administering an agonist (dexmedetomidine) that significantly reduced resting-state functional connectivity both within and between brain subnetworks (Hashmi et al., 2017). The α2 adrenergic tone has a direct link with stress, stress resilience and anxiety (Grueschow et al., 2021; McCall et al., 2015; Ross & Van Bockstaele, 2020). In rodents, stimulant drugs and physiological manipulations targeting these receptors can lead to heightened LC-reactivity to stressors (Morris et al., 2020; Samuels & Szabadi, 2008). The heightened noradrenergic tone following an aversive threat can promote cued fear learning that in turn enhances amygdala function and impairs prefrontal structure and function (Giustino & Maren, 2018). This segues into the observed association between increased SS and higher state and trait anxiety and higher magnification, a subscale of pain catastrophizing. Previous studies have linked increased anxiety to decreased resting-state functional connectivity within/between the affective (AN), salience (SN), central executive (CEN) and default mode (DMN) networks (Xu et al., 2019). Excessive anxiety has been associated with lower functional connectivity between the DMN and the anterior SN (Gerlach et al., 2021). Since pain is an aversive signal, pain processes and aversive fear conditioning share similar pathways (Biggs et al., 2020; Ceko et al., 2022; Elman & Borsook, 2018; Ji et al., 2018). The observed association between SS, threat bias, and anxiety prone behaviors taken together with what has been suggested about a role of adrenergic pathways in arousal and network integration suggests a role of altered autonomic nervous system function in fear of pain. In addition, the SS measure offers a global metric that can be investigated to study the putative link between adrenergic (and potentially other neurotransmitters) tone (Shine, 2019;

Shine et al., 2018; Shine et al., 2019) and anxiety prone patterns of responses to pain (Delgado-Gallén et al., 2023).

Previous work from our lab also indicates that white matter pathways that connect disparate brain regions show reduced integrity in people with high threat bias (Aristi et al., 2022). Specifically, people with high threat bias exhibit weaknesses in the splenium of the corpus collosum (Aristi et al., 2022). This region is a structural pathway that connects sensory regions with multimodal regions in parietal cortex and is important for integrating top-down information with bottom-up sensory input (Aristi et al., 2022; Fabri et al., 2001). We conclude that individual differences behind macroscale and microscale neurophysiological mechanisms account for variation in threat bias sensitivity and can be reflected in measures of large-scale functional dynamics such as SS.

We found that participants in the high bias group showed significant change in SS from rest-to-task while networks in individuals from the low bias group stayed consistently integrated across all scans. Several studies reported that large-scale brain networks stay less integrated during task performance compared to rest (Cohen & D'Esposito, 2016; Cole et al., 2014; Krienen et al., 2014; Shine et al., 2016). Whether the system is more integrated or segregated depends on task complexity that requires different amount of cognitive control: simple tasks are associated with greater network segregation, while more complex tasks favor decreased segregation (Cohen & D'Esposito, 2016; Shine et al., 2016; Yue et al., 2017). These rest-to-task differences in segregation can be explained by the need to minimize metabolic cost of brain function (Bullmore & Sporns, 2012; Zalesky et al., 2014). Brain networks are wired to minimize metabolic costs by staying less

clustered / more segregated at rest, but task-related processing demands engage communication and relocation of energy resources between specific task-relevant networks that become more connected / integrated (Bullmore & Sporns, 2012). Our results suggest that the high bias group required greater engagement of brain networks sub-serving greater cognitive efforts to integrate prior expectations and contradictory sensory stimuli and thus demonstrated higher variation in task-specific network organization across the scans. Given that these changes across rest vs task conditions are specific to certain types of people, individual variation in network architecture may be related to cognitive ability and these assertions need confirmation.

Our results were produced based on two different cortical parcellations that involve known canonical RSNs. The seven and seventeen networks in the Yeo parcellations are two subscale resolutions of brain regions that show high reproducibility of resting-state fMRI connectivity when assessed from a thousand subjects (Yeo et al., 2011). Parcellations derived from large groups of healthy individuals have provided important insights into study of brain topological organization and network properties (Buckner et al., 2013). These properties have allowed researchers to investigate brain behavioural associations with developmental, cognitive, and behavioural phenotypes. It has been shown that the size, location, and spatial arrangement albeit consistent between subjects, does show individual level variations (Braga & Buckner, 2017; Harrison et al., 2015; Laumann et al., 2015). Yet, it remains unclear whether topological metrics derived from subject-specific parcellations are comparable in their association with behavior relative to metrics from group-based parcellations (Hacker et al., 2013; Wig et al., 2014). Here, we tested the possibility of whether individual-specific network organization offers comparable information to group-averaged networks. We showed that segregation in the predefined five and seven RSNs was

more robust in association with pain behavior. The higher resolution parcellations with seventeen RSNs showed some correspondence but was less predictive relative to the spatially coarser resolution networks, and segregation in individual-specific RSNs obtained by Girvan-Newman and Louvain algorithms failed to predict threat bias. Overall, our results indicate that predefined group-averaged RSNs are better at capturing behavioral differences associated with threat bias in pain compared to subject-specific RSNs.

The main limitation of this study is the absence of a validation data set to test the reproducibility of current findings. The small group sizes resulting from the K-means clustering algorithm may reduce the statistical power of group analyses. Nonetheless, our data provided sufficient power to establish neurobiological correlates of top-down threat bias in pain observable in resting-state fMRI. As we demonstrated, the choice of parcellation, spatial resolution of the parcellation and type of scan (rest vs task) lead to different results. Thus, a more thorough investigation of variables with larger dataset and cognitive measurements can help to validate and extend the findings.

In summary, this study shows, for the first time, that segregation in canonical RSNs is a predictive of individual variance in threat bias. Specifically, we suggest the balance between large scale dynamics in RSNs is critical for the processes involved in integrating sensory information with top-down priors in response to threat. Increased SS is also related to maladaptive pain traits such as higher pain catastrophizing and increased pain responsiveness to threat. Therefore, higher integration may be an indicator of coordinated activity between multiple brain networks that allows proper sensory integration and reduced amplification of sensory responses to threats. Future work

that focuses on further investigation of neurobiological mechanisms implicated in top-down cognitive biases in pain can benefit the development of interventions targeting chronic pain conditions.

ACKNOWLEDGHMENTS

Data Availability Statement: The data that support the findings of this study are available from the corresponding author upon request.

Funding Statement: This study was funded the Natural Sciences and Research Engineering Council of Canada (NSERC) Discovery Grant, the Canada Research Chairs Program, the John R. Evans Leaders and Canada Innovation Funds (CFI-JELF), the Canadian Institute of Health Research (CIHR) Project Grant, the Nova Scotia Health Authority (NSHA) Establishment Grant, and the NSHA Fibromyalgia Research Grant.

Conflict of Interest Disclosure: The authors have no conflicts of interest to declare.

References

Aristi, G., O'Grady, C., Bowen, C., Beyea, S., Lazar, S. W., & Hashmi, J. A. (2022). Top-down threat bias in pain perception is predicted by intrinsic structural and functional connections of the brain. *Neuroimage*, 119349. https://doi.org/10.1016/j.neuroimage.2022.119349

Arnemann, K. L., Chen, A. J., Novakovic-Agopian, T., Gratton, C., Nomura, E. M., & D'Esposito, M. (2015). Functional brain network modularity predicts response to cognitive training after brain injury. *Neurology*, *84*(15), 1568-1574. https://doi.org/10.1212/WNL.0000000000001476

Aue, T., & Okon-Singer, H. (2015). Expectancy biases in fear and anxiety and their link to biases in attention. *Clin Psychol Rev*, *42*, 83-95. https://doi.org/10.1016/j.cpr.2015.08.005

Avena-Koenigsberger, A., Misic, B., & Sporns, O. (2017). Communication dynamics in complex brain networks. *Nat Rev Neurosci*, *19*(1), 17-33. https://doi.org/10.1038/nrn.2017.149

Baniqued, P. L., Gallen, C. L., Kranz, M. B., Kramer, A. F., & D'Esposito, M. (2019). Brain network modularity predicts cognitive training-related gains in young adults. *Neuropsychologia*, *131*, 205-215. https://doi.org/10.1016/j.neuropsychologia.2019.05.021

Baniqued, P. L., Gallen, C. L., Voss, M. W., Burzynska, A. Z., Wong, C. N., Cooke, G. E., Duffy, K., Fanning, J., Ehlers, D. K., Salerno, E. A., Aguinaga, S., McAuley, E., Kramer, A. F., & D'Esposito, M. (2017). Brain Network Modularity Predicts Exercise-Related Executive Function Gains in Older Adults. *Front Aging Neurosci*, *9*, 426. https://doi.org/10.3389/fnagi.2017.00426

Bar-Haim, Y., Lamy, D., Pergamin, L., Bakermans-Kranenburg, M. J., & van, I. M. H. (2007). Threat-related attentional bias in anxious and nonanxious individuals: a meta-analytic study. *Psychol Bull*, *133*(1), 1-24. https://doi.org/10.1037/0033-2909.133.1.1

Baum, G. L., Ciric, R., Roalf, D. R., Betzel, R. F., Moore, T. M., Shinohara, R. T., Kahn, A. E., Vandekar, S. N., Rupert, P. E., Quarmley, M., Cook, P. A., Elliott, M. A., Ruparel, K., Gur, R. E., Gur, R. C., Bassett, D. S., & Satterthwaite, T. D. (2017). Modular Segregation of Structural Brain Networks Supports the Development of Executive Function in Youth. *Curr Biol*, *27*(11), 1561-1572 e1568. https://doi.org/10.1016/j.cub.2017.04.051

Biggs, E. E., Timmers, I., Meulders, A., Vlaeyen, J. W. S., Goebel, R., & Kaas, A. L. (2020). The neural correlates of pain-related fear: A meta-analysis comparing fear conditioning studies using painful and non-painful stimuli. *Neurosci Biobehav Rev*, *119*, 52-65. https://doi.org/10.1016/j.neubiorev.2020.09.016

Blondel, V. D., Guillaume, J.-L., Lambiotte, R., & Lefebvre, E. (2008). Fast unfolding of communities in large networks. *Journal of Statistical Mechanics: Theory and Experiment*, *2008*(10). https://doi.org/10.1088/1742-5468/2008/10/p10008

Braga, R. M., & Buckner, R. L. (2017). Parallel Interdigitated Distributed Networks within the Individual Estimated by Intrinsic Functional Connectivity. *Neuron*, *95*(2), 457-471 e455. https://doi.org/10.1016/j.neuron.2017.06.038

Buckner, R. L., Krienen, F. M., & Yeo, B. T. (2013). Opportunities and limitations of intrinsic functional connectivity MRI. *Nat Neurosci*, *16*(7), 832-837. https://doi.org/10.1038/nn.3423

Bullmore, E., & Sporns, O. (2012). The economy of brain network organization. *Nat Rev Neurosci*, *13*(5), 336-349. https://doi.org/10.1038/nrn3214

Caras, M. L., & Sanes, D. H. (2017). Top-down modulation of sensory cortex gates perceptual learning. *Proc Natl Acad Sci U S A*, *114*(37), 9972-9977. https://doi.org/10.1073/pnas.1712305114

Ceko, M., Kragel, P. A., Woo, C. W., Lopez-Sola, M., & Wager, T. D. (2022). Common and stimulus-type-specific brain representations of negative affect. *Nat Neurosci*, *25*(6), 760-770. https://doi.org/10.1038/s41593-022-01082-w

Chan, M. Y., Park, D. C., Savalia, N. K., Petersen, S. E., & Wig, G. S. (2014). Decreased segregation of brain systems across the healthy adult lifespan. *Proc Natl Acad Sci U S A*, *111*(46), E4997-5006. https://doi.org/10.1073/pnas.1415122111

Choi, I., Lee, J. Y., & Lee, S. H. (2018). Bottom-up and top-down modulation of multisensory integration. *Curr Opin Neurobiol*, *52*, 115-122. https://doi.org/10.1016/j.conb.2018.05.002

Cohen, J. R., & D'Esposito, M. (2016). The Segregation and Integration of Distinct Brain Networks and Their Relationship to Cognition. *J Neurosci*, *36*(48), 12083-12094. https://doi.org/10.1523/JNEUROSCI.2965-15.2016

Cole, M. W., Bassett, D. S., Power, J. D., Braver, T. S., & Petersen, S. E. (2014). Intrinsic and task-evoked network architectures of the human brain. *Neuron*, *83*(1), 238-251. https://doi.org/10.1016/j.neuron.2014.05.014

Deco, G., Tononi, G., Boly, M., & Kringelbach, M. L. (2015). Rethinking segregation and integration: contributions of whole-brain modelling. *Nat Rev Neurosci*, *16*(7), 430-439. https://doi.org/10.1038/nrn3963

Delgado-Gallén, S., Soler, M. D., Cabello-Toscano, M., Abellaneda-Pérez, K., Solana-Sánchez, J., España-Irla, G., Roca-Ventura, A., Bartrés-Faz, D., Tormos, J. M., Pascual-Leone, A., & Cattaneo, G. (2023). Brain system segregation and pain catastrophizing in chronic pain progression. *Front Neurosci*, *17*, 1148176. https://doi.org/10.3389/fnins.2023.1148176

Drakesmith, M., Caeyenberghs, K., Dutt, A., Lewis, G., David, A. S., & Jones, D. K. (2015). Overcoming the effects of false positives and threshold bias in graph theoretical analyses of neuroimaging data. *Neuroimage*, *118*, 313-333. https://doi.org/10.1016/j.neuroimage.2015.05.011

Elman, I., & Borsook, D. (2018). Threat Response System: Parallel Brain Processes in Pain vis-à-vis Fear and Anxiety. *Front Psychiatry*, *9*, 29. https://doi.org/10.3389/fpsyt.2018.00029

Fabri, M., Polonara, G., Del Pesce, M., Quattrini, A., Salvolini, U., & Manzoni, T. (2001). Posterior corpus callosum and interhemispheric transfer of somatosensory information: an fMRI and neuropsychological study of a partially callosotomized patient. *J Cogn Neurosci*, *13*(8), 1071-1079. https://doi.org/10.1162/089892901753294365

Fields, H. L. (2018). How expectations influence pain. *Pain*, *159 Suppl 1*, S3-S10. https://doi.org/10.1097/j.pain.0000000000001272

Fonov, V., Evans, A. C., Botteron, K., Almli, C. R., McKinstry, R. C., & Collins, D. L. (2011). Unbiased average age-appropriate atlases for pediatric studies. *Neuroimage*, *54*(1), 313-327. https://doi.org/10.1016/j.neuroimage.2010.07.033

Friston, K. J. (2009). Modalities, Modes, and Models in Functional Neuroimaging. *Science*, *326*(5951), 399-403. https://doi.org/10.1126/science.1174521

Gallen, C. L., Baniqued, P. L., Chapman, S. B., Aslan, S., Keebler, M., Didehbani, N., & D'Esposito, M. (2016). Modular Brain Network Organization Predicts Response to Cognitive Training in Older Adults. *PLoS One*, *11*(12), e0169015. https://doi.org/10.1371/journal.pone.0169015

Gerlach, A. R., Karim, H. T., Kazan, J., Aizenstein, H. J., Krafty, R. T., & Andreescu, C. (2021). Networks of worry-towards a connectivity-based signature of late-life worry using higher criticism. *Transl Psychiatry*, *11*(1), 550. https://doi.org/10.1038/s41398-021-01648-5

Giustino, T. F., & Maren, S. (2018). Noradrenergic Modulation of Fear Conditioning and Extinction. *Front Behav Neurosci*, *12*, 43. https://doi.org/10.3389/fnbeh.2018.00043

Gozdas, E., Holland, S. K., Altaye, M., & Consortium, C. A. (2019). Developmental changes in functional brain networks from birth through adolescence. *Hum Brain Mapp*, *40*(5), 1434-1444. https://doi.org/10.1002/hbm.24457

Grueschow, M., Stenz, N., Thorn, H., Ehlert, U., Breckwoldt, J., Brodmann Maeder, M., Exadaktylos, A. K., Bingisser, R., Ruff, C. C., & Kleim, B. (2021). Real-world stress resilience is associated with the responsivity of the locus coeruleus. *Nat Commun*, *12*(1), 2275. https://doi.org/10.1038/s41467-021-22509-1

Hacker, C. D., Laumann, T. O., Szrama, N. P., Baldassarre, A., Snyder, A. Z., Leuthardt, E. C., & Corbetta, M. (2013). Resting state network estimation in individual subjects. *Neuroimage*, *82*, 616-633. https://doi.org/10.1016/j.neuroimage.2013.05.108

Harrison, S. J., Woolrich, M. W., Robinson, E. C., Glasser, M. F., Beckmann, C. F., Jenkinson, M., & Smith, S. M. (2015). Large-scale probabilistic functional modes from resting state fMRI. *Neuroimage*, *109*, 217-231. https://doi.org/10.1016/j.neuroimage.2015.01.013

Hashmi, J. A., Kong, J., Spaeth, R., Khan, S., Kaptchuk, T. J., & Gollub, R. L. (2014). Functional network architecture predicts psychologically mediated analgesia related to treatment in chronic knee pain patients. *J Neurosci*, *34*(11), 3924-3936. https://doi.org/10.1523/JNEUROSCI.3155-13.2014

Hashmi, J. A., Loggia, M. L., Khan, S., Gao, L., Kim, J., Napadow, V., Brown, E. N., & Akeju, O. (2017). Dexmedetomidine Disrupts the Local and Global Efficiencies of Large-scale Brain Networks. *Anesthesiology*, *126*(3), 419-430. https://doi.org/10.1097/ALN.0000000000001509

Heathcote, L. C., Timmers, I., Kronman, C. A., Mahmud, F., Hernandez, J. M., Bentley, J., Youssef, A. M., Pine, D. S., Borsook, D., & Simons, L. E. (2020). Brain signatures of threat-safety discrimination in adolescent chronic pain. *Pain*, *161*(3), 630-640. https://doi.org/10.1097/j.pain.0000000000001753

Ji, G., Yakhnitsa, V., Kiritoshi, T., Presto, P., & Neugebauer, V. (2018). Fear extinction learning ability predicts neuropathic pain behaviors and amygdala activity in male rats. *Mol Pain*, *14*, 1744806918804441. https://doi.org/10.1177/1744806918804441

Kelley, N. J., & Schmeichel, B. J. (2014). The effects of negative emotions on sensory perception: fear but not anger decreases tactile sensitivity. *Front Psychol*, *5*, 942. https://doi.org/10.3389/fpsyg.2014.00942

Khan, S., Hashmi, J. A., Mamashli, F., Hamalainen, M. S., & Kenet, T. (2022). Functional Significance of Human Resting-State Networks Hubs Identified Using MEG During the Transition From Childhood to Adulthood. *Front Neurol*, *13*, 814940. https://doi.org/10.3389/fneur.2022.814940

Kong, J., Jensen, K., Loiotile, R., Cheetham, A., Wey, H. Y., Tan, Y., Rosen, B., Smoller, J. W., Kaptchuk, T. J., & Gollub, R. L. (2013). Functional connectivity of the frontoparietal network predicts cognitive modulation of pain. *Pain*, *154*(3), 459-467. https://doi.org/10.1016/j.pain.2012.12.004

Krienen, F. M., Yeo, B. T., & Buckner, R. L. (2014). Reconfigurable task-dependent functional coupling modes cluster around a core functional architecture. *Philos Trans R Soc Lond B Biol Sci*, *369*(1653). https://doi.org/10.1098/rstb.2013.0526

Kucyi, A., & Davis, K. D. (2015). The dynamic pain connectome. *Trends Neurosci*, *38*(2), 86-95. https://doi.org/10.1016/j.tins.2014.11.006

Laumann, T. O., Gordon, E. M., Adeyemo, B., Snyder, A. Z., Joo, S. J., Chen, M. Y., Gilmore, A. W., McDermott, K. B., Nelson, S. M., Dosenbach, N. U., Schlaggar, B. L., Mumford, J. A., Poldrack, R. A., & Petersen, S. E. (2015). Functional System and Areal Organization of a Highly Sampled Individual Human Brain. *Neuron*, *87*(3), 657-670. https://doi.org/10.1016/j.neuron.2015.06.037

LeDoux, J. E. (2014). Coming to terms with fear. *Proc Natl Acad Sci U S A*, *111*(8), 2871-2878. https://doi.org/10.1073/pnas.1400335111

Leeuw, M., Goossens, M. E., Linton, S. J., Crombez, G., Boersma, K., & Vlaeyen, J. W. (2007). The fear-avoidance model of musculoskeletal pain: current state of scientific evidence. *J Behav Med*, *30*(1), 77-94. https://doi.org/10.1007/s10865-006-9085-0

Legrain, V., Iannetti, G. D., Plaghki, L., & Mouraux, A. (2011). The pain matrix reloaded: a salience detection system for the body. *Prog Neurobiol*, *93*(1), 111-124. https://doi.org/10.1016/j.pneurobio.2010.10.005

Lim, M., O'Grady, C., Cane, D., Goyal, A., Lynch, M., Beyea, S., & Hashmi, J. A. (2020). Threat Prediction from Schemas as a Source of Bias in Pain Perception. *J Neurosci*, *40*(7), 1538-1548. https://doi.org/10.1523/JNEUROSCI.2104-19.2019

Lloyd, S. P. (1982). Least squares quantization in PCM. *IEEE Trans. Inf. Theory*, *28*, 129-136.

McCall, J. G., Al-Hasani, R., Siuda, E. R., Hong, D. Y., Norris, A. J., Ford, C. P., & Bruchas, M. R. (2015). CRH Engagement of the Locus Coeruleus Noradrenergic System Mediates Stress-Induced Anxiety. *Neuron*, *87*(3), 605-620. https://doi.org/10.1016/j.neuron.2015.07.002

Misic, B., & Sporns, O. (2016). From regions to connections and networks: new bridges between brain and behavior. *Curr Opin Neurobiol*, *40*, 1-7. https://doi.org/10.1016/j.conb.2016.05.003

Morris, L. S., McCall, J. G., Charney, D. S., & Murrough, J. W. (2020). The role of the locus coeruleus in the generation of pathological anxiety. *Brain Neurosci Adv*, *4*, 2398212820930321. https://doi.org/10.1177/2398212820930321

Newman, M. E., & Girvan, M. (2004). Finding and evaluating community structure in networks. *Phys Rev E Stat Nonlin Soft Matter Phys*, *69*(2 Pt 2), 026113. https://doi.org/10.1103/PhysRevE.69.026113

Peters, M. L., Vlaeyen, J. W., & Kunnen, A. M. (2002). Is pain-related fear a predictor of somatosensory hypervigilance in chronic low back pain patients? *Behav Res Ther*, *40*(1), 85-103. http://www.ncbi.nlm.nih.gov/pubmed/11764761

Ross, J. A., & Van Bockstaele, E. J. (2020). The Locus Coeruleus- Norepinephrine System in Stress and Arousal: Unraveling Historical, Current, and Future Perspectives. *Front Psychiatry*, *11*, 601519. https://doi.org/10.3389/fpsyt.2020.601519

Rubinov, M., & Sporns, O. (2010). Complex network measures of brain connectivity: uses and interpretations. *Neuroimage*, *52*(3), 1059-1069. https://doi.org/10.1016/j.neuroimage.2009.10.003

Saghayi, M., Greenberg, J., O'Grady, C., Varno, F., Hashmi, M. A., Bracken, B., Matwin, S., Lazar, S. W., & Hashmi, J. A. (2020). Brain network topology predicts participant

adherence to mental training programs. *Netw Neurosci*, *4*(3), 528-555. https://doi.org/10.1162/netn_a_00136
Samuels, E. R., & Szabadi, E. (2008). Functional neuroanatomy of the noradrenergic locus coeruleus: its roles in the regulation of arousal and autonomic function part I: principles of functional organisation. *Curr Neuropharmacol*, *6*(3), 235-253. https://doi.org/10.2174/157015908785777229
Shine, J. M. (2019). Neuromodulatory Influences on Integration and Segregation in the Brain. *Trends Cogn Sci*, *23*(7), 572-583. https://doi.org/10.1016/j.tics.2019.04.002
Shine, J. M., Aburn, M. J., Breakspear, M., & Poldrack, R. A. (2018). The modulation of neural gain facilitates a transition between functional segregation and integration in the brain. *eLife*, *7*. https://doi.org/10.7554/eLife.31130
Shine, J. M., Bissett, P. G., Bell, P. T., Koyejo, O., Balsters, J. H., Gorgolewski, K. J., Moodie, C. A., & Poldrack, R. A. (2016). The Dynamics of Functional Brain Networks: Integrated Network States during Cognitive Task Performance. *Neuron*, *92*(2), 544-554. https://doi.org/10.1016/j.neuron.2016.09.018
Shine, J. M., Breakspear, M., Bell, P. T., Ehgoetz Martens, K. A., Shine, R., Koyejo, O., Sporns, O., & Poldrack, R. A. (2019). Human cognition involves the dynamic integration of neural activity and neuromodulatory systems. *Nat Neurosci*, *22*(2), 289-296. https://doi.org/10.1038/s41593-018-0312-0
Smith, R., Badcock, P., & Friston, K. J. (2021). Recent advances in the application of predictive coding and active inference models within clinical neuroscience. *Psychiatry Clin Neurosci*, *75*(1), 3-13. https://doi.org/10.1111/pcn.13138
Spielberger, C. D., Gorsuch, R. L., & Lushene, R. E. (1970). Manual for the State-Trait Anxiety Inventory.
Sporns, O. (2013). Network attributes for segregation and integration in the human brain. *Curr Opin Neurobiol*, *23*(2), 162-171. https://doi.org/10.1016/j.conb.2012.11.015
Sporns, O., & Betzel, R. F. (2016). Modular Brain Networks. *Annu Rev Psychol*, *67*, 613-640. https://doi.org/10.1146/annurev-psych-122414-033634
Sullivan, M. J. L., Bishop, S. R., & Pivik, J. (1995). The Pain Catastrophizing Scale: Development and validation. *Psychological Assessment*, *7*(4), 524-532. https://doi.org/10.1037//1040-3590.7.4.524
van den Heuvel, M. P., de Lange, S. C., Zalesky, A., Seguin, C., Yeo, B. T. T., & Schmidt, R. (2017). Proportional thresholding in resting-state fMRI functional connectivity networks and consequences for patient-control connectome studies: Issues and recommendations. *Neuroimage*, *152*, 437-449. https://doi.org/10.1016/j.neuroimage.2017.02.005
van den Heuvel, M. P., & Sporns, O. (2013). Network hubs in the human brain. *Trends Cogn Sci*, *17*(12), 683-696. https://doi.org/10.1016/j.tics.2013.09.012
van Wijk, B. C., Stam, C. J., & Daffertshofer, A. (2010). Comparing brain networks of different size and connectivity density using graph theory. *PLoS One*, *5*(10), e13701. https://doi.org/10.1371/journal.pone.0013701
Wainstein, G., Rojas-Libano, D., Medel, V., Alnaes, D., Kolskar, K. K., Endestad, T., Laeng, B., Ossandon, T., Crossley, N., Matar, E., & Shine, J. M. (2021). The ascending arousal system promotes optimal performance through mesoscale network integration in a visuospatial attentional task. *Netw Neurosci*, *5*(4), 890-910. https://doi.org/10.1162/netn_a_00205

Wang, S., Veinot, J., Goyal, A., Khatibi, A., Lazar, S. W., & Hashmi, J. A. (2022). Distinct networks of periaqueductal gray columns in pain and threat processing. *Neuroimage*, *250*, 118936. https://doi.org/10.1016/j.neuroimage.2022.118936

Wig, G. S. (2017). Segregated Systems of Human Brain Networks. *Trends Cogn Sci*, *21*(12), 981-996. https://doi.org/10.1016/j.tics.2017.09.006

Wig, G. S., Laumann, T. O., Cohen, A. L., Power, J. D., Nelson, S. M., Glasser, M. F., Miezin, F. M., Snyder, A. Z., Schlaggar, B. L., & Petersen, S. E. (2014). Parcellating an individual subject's cortical and subcortical brain structures using snowball sampling of resting-state correlations. *Cereb Cortex*, *24*(8), 2036-2054. https://doi.org/10.1093/cercor/bht056

Xu, J., Van Dam, N. T., Feng, C., Luo, Y., Ai, H., Gu, R., & Xu, P. (2019). Anxious brain networks: A coordinate-based activation likelihood estimation meta-analysis of resting-state functional connectivity studies in anxiety. *Neurosci Biobehav Rev*, *96*, 21-30. https://doi.org/10.1016/j.neubiorev.2018.11.005

Yeo, B. T., Krienen, F. M., Sepulcre, J., Sabuncu, M. R., Lashkari, D., Hollinshead, M., Roffman, J. L., Smoller, J. W., Zollei, L., Polimeni, J. R., Fischl, B., Liu, H., & Buckner, R. L. (2011). The organization of the human cerebral cortex estimated by intrinsic functional connectivity. *J Neurophysiol*, *106*(3), 1125-1165. https://doi.org/10.1152/jn.00338.2011

Yue, Q., Martin, R. C., Fischer-Baum, S., Ramos-Nunez, A. I., Ye, F., & Deem, M. W. (2017). Brain Modularity Mediates the Relation between Task Complexity and Performance. *J Cogn Neurosci*, *29*(9), 1532-1546. https://doi.org/10.1162/jocn_a_01142

Zalesky, A., Fornito, A., Cocchi, L., Gollo, L. L., & Breakspear, M. (2014). Time-resolved resting-state brain networks. *Proc Natl Acad Sci U S A*, *111*(28), 10341-10346. https://doi.org/10.1073/pnas.1400181111

Zalesky, A., Fornito, A., Cocchi, L., Gollo, L. L., van den Heuvel, M. P., & Breakspear, M. (2016). Connectome sensitivity or specificity: which is more important? *Neuroimage*, *142*, 407-420. https://doi.org/10.1016/j.neuroimage.2016.06.035

Zhi, D., King, M., Hernandez-Castillo, C. R., & Diedrichsen, J. (2022). Evaluating brain parcellations using the distance-controlled boundary coefficient. *Hum Brain Mapp*. https://doi.org/10.1002/hbm.25878

Figure 1

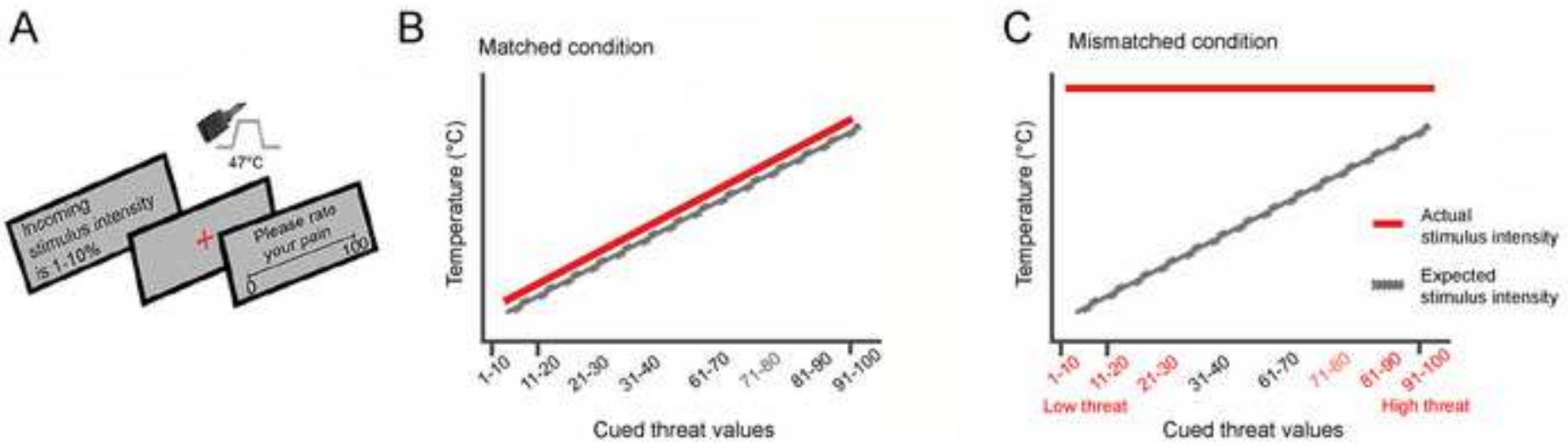

Figure 2

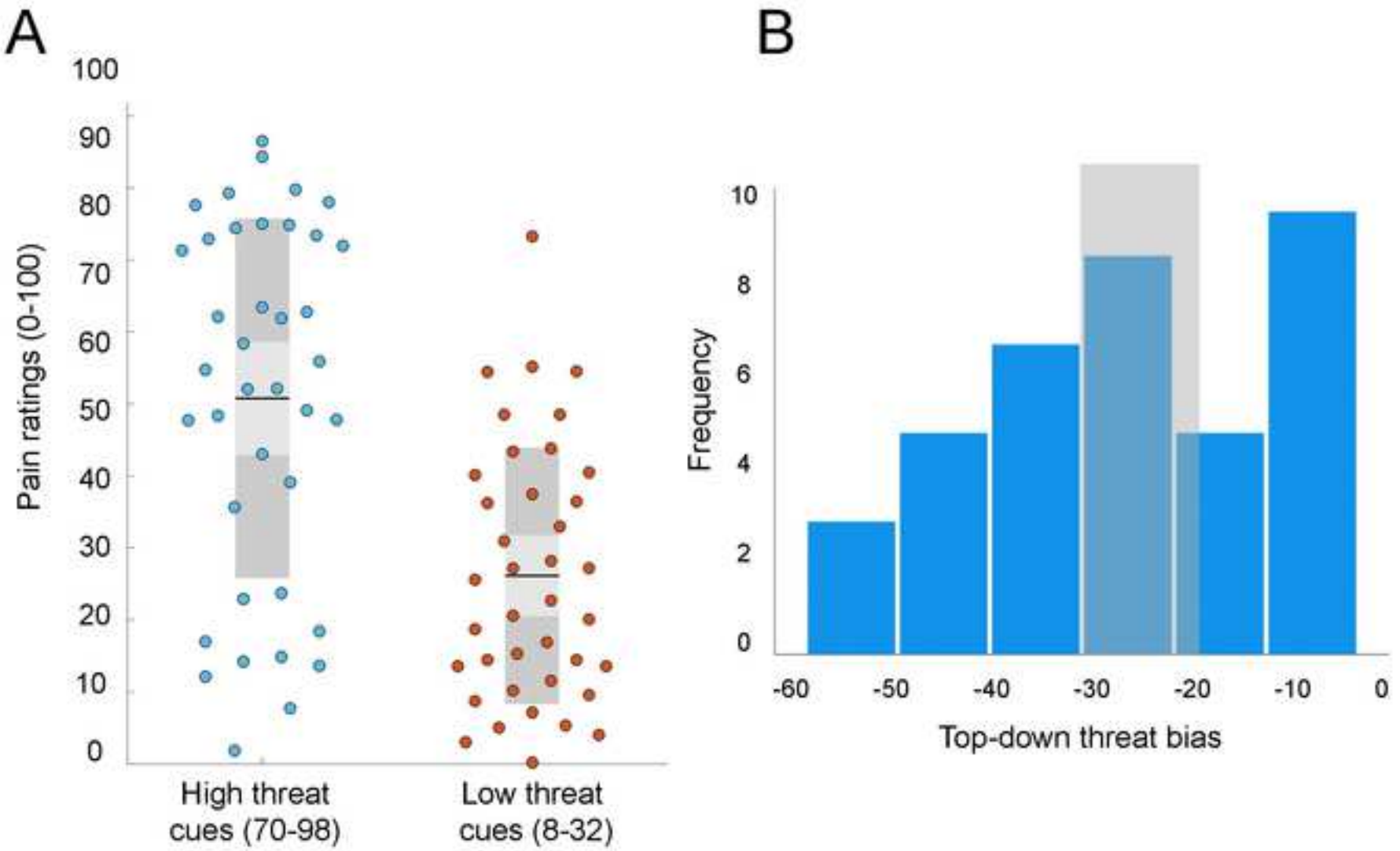

Figure 3

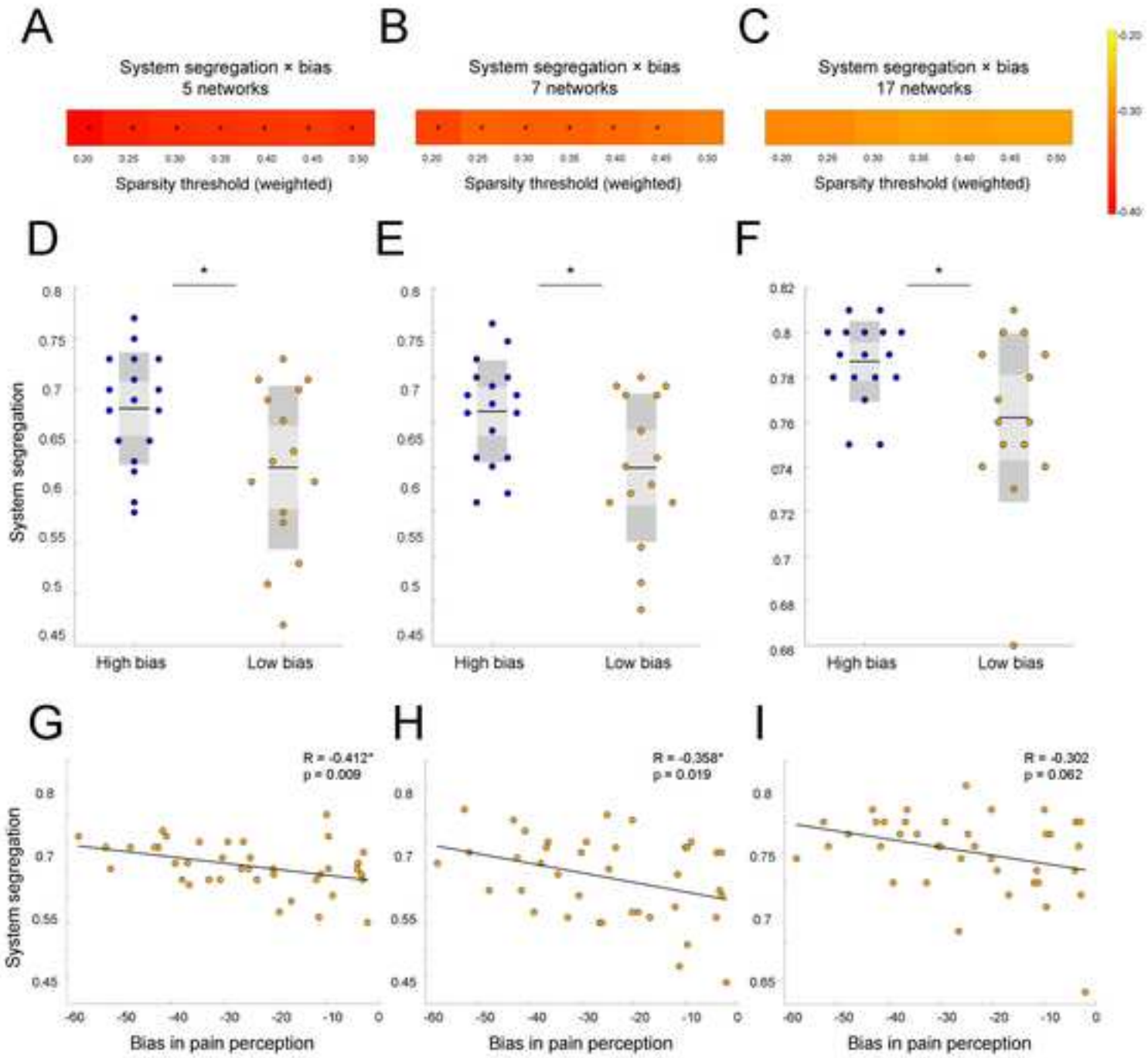

Figure 4

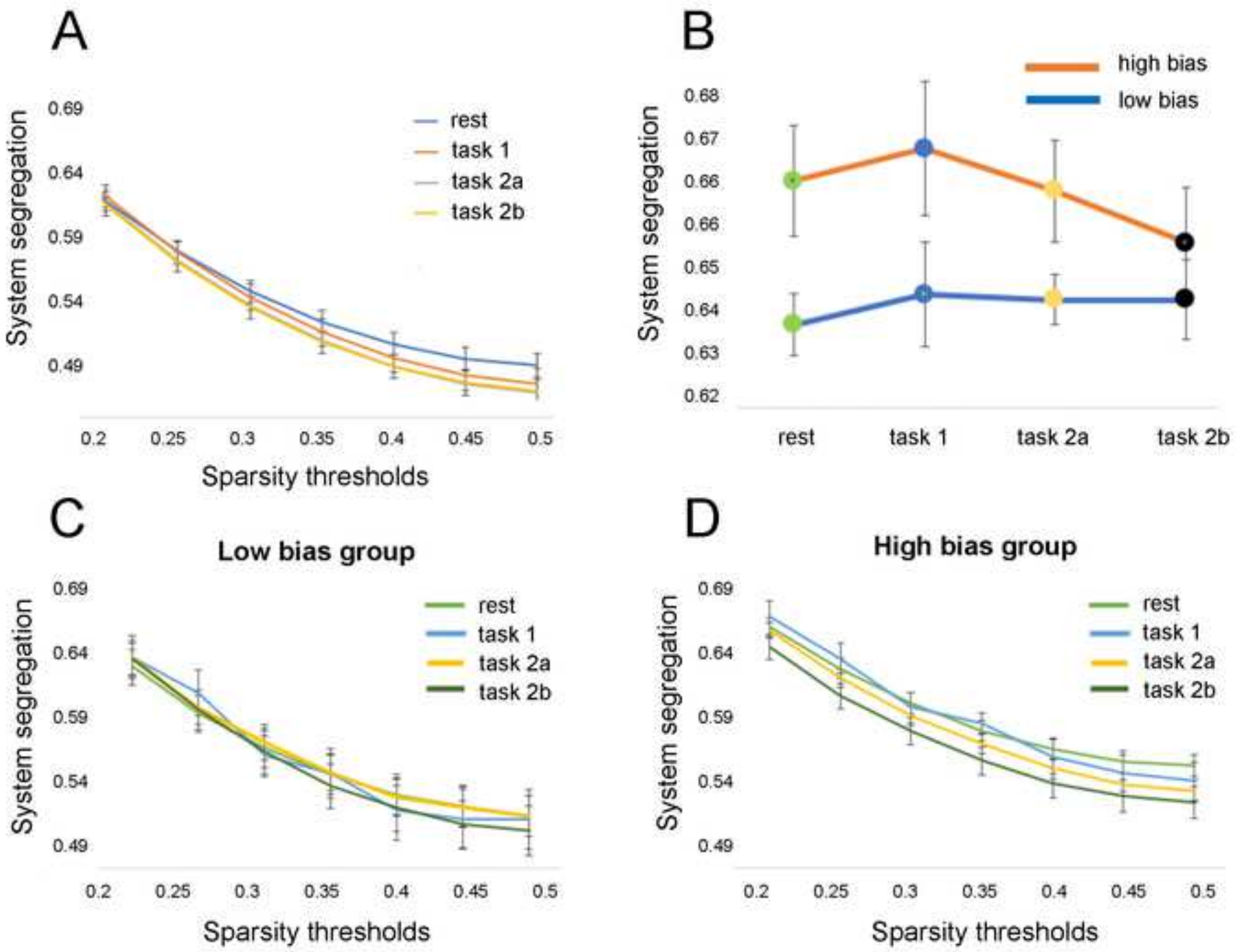

AUTHOR SUMMARY

Some individuals are more sensitive to threats of receiving strong pain stimuli. In this study, we report that higher system segregation in brain networks is associated with a greater threat bias (a reliance on expected intensity of pain versus the actual sensory stimuli in the manipulated pain experiment). We verified the results with different pre-defined resting-state parcellations at different network sparsities, and also tested subject-driven parcellations. These findings demonstrate that higher integration between resting-state networks is conducive for integrating top-down expectation processes with changes in bottom-up noxious stimulus intensities. Network segregation in resting state is thus associated with poor sensory integration and also shows association with anxiety and fear of pain.